

Relaxation time for electron-dislocation scattering for noble and polyvalent metals

A. Bergmann, M. Kaveh,* and N. Wisser

Department of Physics, Bar-Ilan University, Ramat-Gan, Israel

(Received 17 March 1981)

An analysis is presented of the relaxation time for electron-dislocation scattering for the polyvalent and noble metals. It is shown that for these metals the relaxation time is significantly anisotropic, i.e., its magnitude varies markedly with position over the Fermi surface. This anisotropy of the relaxation time results from the nonsphericity of the Fermi surface for these metals and from the dominance of very-small-angle scattering events for electron-dislocation scattering. The explicit form of the relaxation time is determined by a variational solution to the Boltzmann equation. The degree of anisotropy of the relaxation time is calculated for Al, Cu, Ag, and Au. The analysis is then generalized to include the effects of both electron-dislocation scattering and electron-impurity scattering. It is shown that the large-angle scattering events that characterize electron-impurity scattering tend to reduce the anisotropy of the relaxation time. Finally, a discussion is presented of the implications of the present results to the recent theories of the effect of electron-dislocation scattering on the low-temperature electrical resistivity of the polyvalent and noble metals.

I. INTRODUCTION

Over the past few years, it has become recognized that the presence of a significant density of dislocation lines in a metal sample can have a marked effect on the low-temperature electrical resistivity. For example, the magnitude of the temperature-dependent part of the resistivity $\Delta\rho(T)$ depends on the dislocation density N_D present in the sample. It has long been known^{1,2} that $\Delta\rho(T)$ depends on the magnitude of the residual resistivity ρ_0 , an effect known as deviations from Matthiessen's rule. However, in recent years experimental evidence³⁻¹² has been accumulating to show that $\Delta\rho(T)$ also depends on the *source* of ρ_0 .

The explanation for the dependence of $\Delta\rho(T)$ on N_D is the following. The calculation of $\Delta\rho(T)$ depends on the electron distribution function and thus on the relaxation time $\tau(\vec{K})$ for each electron state \vec{K} on the Fermi surface. However, $\tau(\vec{K})$ is determined by *all* electron scattering processes that occur in the sample, including electron-dislocation scattering. In other words, two samples which have the same value of ρ_0 may have quite different values for $\tau(\vec{K})$ if for one sample, ρ_0 arises primarily from electron-impurity scattering, whereas for the other sample, ρ_0 arises primarily from electron-dislocation scattering.

The suggestion that $\tau(\vec{K})$ depends on the source of ρ_0 was proposed by Dugdale and Basinski¹³ and

discussed qualitatively by Rowlands and Woods.⁷ The first quantitative studies of the effect of dislocations on $\tau(\vec{K})$ were carried out by Bergmann, Kaveh, and Wisser^{14,15} for the noble and polyvalent metals and by Kaveh and Wisser¹⁶ for the alkali metals. However, these previous studies concentrated on the calculation of $\Delta\rho(T)$ as a function of N_D ; the form of $\tau(\vec{K})$ was determined empirically. In this paper, we shall present an explicit calculation of the \vec{K} dependence of the relaxation time for electron-dislocation scattering $\tau_{\text{dis}}(\vec{K})$ for the noble and polyvalent metals. The calculation of $\tau_{\text{dis}}(\vec{K})$ is carried out by means of a variational solution of the Boltzmann equation,¹⁷ based on an approximate expression for the transition probability for electron-dislocation scattering. We find that $\tau_{\text{dis}}(\vec{K})$ has a marked \vec{K} dependence and is thus very anisotropic over the Fermi surface. In particular, $\tau_{\text{dis}}(\vec{K})$ is very small in the nonspherical regions of the Fermi surface near the Brillouin zone boundaries. It will be shown that this important result arises from the fact that very-small-angle scattering events dominate electron-dislocation scattering.

From the above discussion, it follows that a realistic calculation of $\tau_{\text{dis}}(\vec{K})$ for the polyvalent and noble metals must take account of the following two features. First, the transition probability for electron-dislocation scattering is dominated by very-small-angle scattering.^{18,19} Secondly, the Fer-

mi surface of noble and polyvalent metals is non-spherical. Although the Fermi surface of a noble or polyvalent metal is overall very nearly spherical, the small nonspherical regions in the immediate vicinity of the intersections of the Fermi surface and the Brillouin-zone boundaries are of the utmost importance to the calculation of $\tau_{\text{dis}}(\vec{\mathbf{K}})$. This situation is very reminiscent of the calculation of $\tau(\vec{\mathbf{K}})$ appropriate to electron-phonon scattering at low temperatures for the polyvalent and noble metals.^{20,21} However, it will be seen that there are important quantitative differences between the $\tau(\vec{\mathbf{K}})$ for electron-dislocation scattering and for electron-phonon scattering at low temperatures.

In Sec. II, a discussion is presented of the general properties of the relaxation time for electron-dislocation scattering, and a one-parameter functional form is introduced. In Sec. III, it is shown how the value of the parameter is determined for any given polyvalent or noble metal. The calculation is carried out for Al and for all the noble metals. The analysis is generalized in Sec. IV by including the effect of electron-impurity scattering on the relaxation time. The calculated relaxation times for Al and Ag samples are compared with previous empirical determinations. In Sec. V, the implications of the present results are discussed with regard to the low-temperature electron-phonon and electron-electron scattering contributions to the electrical resistivity. The summary follows in Sec. VI.

II. RELAXATION TIME

The most convenient framework for calculating the electron relaxation time for electron-dislocation scattering $\tau_{\text{dis}}(\vec{\mathbf{K}})$ is the variational formulation of the Boltzmann equation.¹⁷ This powerful theoretical tool enables one to obtain a reliable approximation to $\tau_{\text{dis}}(\vec{\mathbf{K}})$ by means of a calculation that includes a realistic description of the Fermi surface of the metal and of the electron-dislocation scatter-

ing transition probability.

We begin by writing the expression for the deviation $\phi(\vec{\mathbf{K}})$, caused by unit electric field \hat{E} , of the electron distribution function from its equilibrium value,¹⁷

$$\phi(\vec{\mathbf{K}}) = -e\tau_{\text{dis}}(\vec{\mathbf{K}})\vec{v}(\vec{\mathbf{K}})\cdot\hat{E}, \quad (2.1)$$

where $\vec{v}(\vec{\mathbf{K}})$ is the velocity of the electron in state $\vec{\mathbf{K}}$. The subscript dis on $\tau_{\text{dis}}(\vec{\mathbf{K}})$ indicates that we are considering a sample for which the dominant scattering process is electron-dislocation scattering. This applies, for example, to a strained sample at low temperatures. The interest in measuring the resistivity at low temperatures is threefold. First, the electron-electron scattering contribution is observable only at very low temperatures. Second, at low temperatures, the electron-phonon scattering contribution has a complex, and hence interesting, temperature dependence. Third, the deviations from Matthiessen's rule are very large at low temperatures. At these low temperatures, the dominant contribution to the resistivity is ρ_0 , which thus determines the form of $\tau(\vec{\mathbf{K}})$. Since we are here considering a strained sample, electron-dislocation scattering dominates electron-impurity scattering and thus the appropriate electron relaxation time for the sample is $\tau_{\text{dis}}(\vec{\mathbf{K}})$.

It should be mentioned that no approximation is involved in writing (2.1). Even though the concept of a "relaxation time" is not always strictly valid,²² it is always possible to express $\phi(\vec{\mathbf{K}})$ in the form (2.1) and use the variational method to determine the function $\tau_{\text{dis}}(\vec{\mathbf{K}})$. Exactly under what circumstances one may interpret the resulting $\vec{\mathbf{K}}$ -dependent function $\tau_{\text{dis}}(\vec{\mathbf{K}})$ as a relaxation time is a complex question that need not concern us here. In the present context, it is simply a matter of convenient terminology that we refer to the function $\tau_{\text{dis}}(\vec{\mathbf{K}})$ as an "anisotropic relaxation time."

The variational expression¹⁷ for the contribution to the electrical resistivity due to electron-dislocation scattering ρ_{dis} is given by

$$\rho_{\text{dis}} = \frac{A \int \int [ds(\vec{\mathbf{K}}_1)/v(\vec{\mathbf{K}}_1)][ds(\vec{\mathbf{K}}_2)/v(\vec{\mathbf{K}}_2)][\phi(\vec{\mathbf{K}}_2) - \phi(\vec{\mathbf{K}}_1)]^2 P_{\text{dis}}(\vec{\mathbf{K}}_1, \vec{\mathbf{K}}_2)}{\left[\int ds(\vec{\mathbf{K}})\vec{v}(\vec{\mathbf{K}})\phi(\vec{\mathbf{K}}) \right]^2}, \quad (2.2)$$

where A is a known constant and the wave vectors $\vec{\mathbf{K}}_1$ and $\vec{\mathbf{K}}_2$ characterize the initial and final electron states, respectively, of the electron being scattered by a dislocation with transition probability

$P_{\text{dis}}(\vec{\mathbf{K}}_1, \vec{\mathbf{K}}_2)$. The surface integrals are to be evaluated over the anisotropic Fermi surface of the polyvalent or noble metal.

The variation theorem states¹⁷ that the function

$\phi(\vec{\mathbf{K}})$ that solves the Boltzmann equation will yield a minimum value for the right-hand side RHS of (2.2). The procedure for finding $\phi(\vec{\mathbf{K}})$ is the following. One assumes a parametrized form for $\tau_{\text{dis}}(\vec{\mathbf{K}})$, and hence $\phi(\vec{\mathbf{K}})$, and then evaluates (2.2) to obtain ρ_{dis} as a function of the parameter (or parameters). The value of the parameter that minimizes ρ_{dis} gives the best choice for $\tau_{\text{dis}}(\vec{\mathbf{K}})$ from among the family of functions that was assumed. The result will of course not be exact, but it should be a reliable approximation to the exact $\tau_{\text{dis}}(\vec{\mathbf{K}})$ if the parametrized form was chosen with care. In particular, it is extremely important to incorporate into the parametrized form assumed for $\tau_{\text{dis}}(\vec{\mathbf{K}})$ all the physical features which the exact $\tau_{\text{dis}}(\vec{\mathbf{K}})$ must possess.

One may deduce a parametrized form for $\tau_{\text{dis}}(\vec{\mathbf{K}})$ which has the correct qualitative behavior by means of a calculation of ρ_{dis} based on the *incorrect* assumption of a $\vec{\mathbf{K}}$ -independent $\tau_{\text{dis}}(\vec{\mathbf{K}})$, to be denoted τ_0 . The integrand of the numerator of ρ_{dis} in (2.2) contains the factor, to be denoted $(\Delta\phi)^2$,

$$(\Delta\phi)^2 \equiv [\phi(\vec{\mathbf{K}}_2) - \phi(\vec{\mathbf{K}}_1)]^2. \quad (2.3)$$

Inserting (2.1) into (2.3) with $\tau_{\text{dis}}(\vec{\mathbf{K}}) = \tau_0$ and averaging over the electric field direction, as is permitted for a cubic crystal, yields

$$(\Delta\phi)^2 = \frac{1}{3} (e\tau_0)^2 [\vec{v}(\vec{\mathbf{K}}_2) - \vec{v}(\vec{\mathbf{K}}_1)]^2. \quad (2.4)$$

For the nearly spherical portions of the Fermi surface, one may use the one-plane-wave (1-PW) expression $\vec{v}_{1\text{-PW}}(\vec{\mathbf{K}}) = \hbar\vec{\mathbf{K}}/m$. Inserting this expression for $\vec{v}(\vec{\mathbf{K}})$ into (2.4) yields

$$(\Delta\phi)_{1\text{-PW}}^2 = \frac{1}{3} (e\hbar\tau_0/m)^2 q^2, \quad (2.5)$$

where $q = |\vec{\mathbf{K}}_2 - \vec{\mathbf{K}}_1|$. On the other hand, for $\vec{\mathbf{K}}$ in the nonspherical portion of the Fermi surface, near the intersections with the Brillouin-zone boundaries, a single plane wave is no longer an adequate representation of the pseudo-wave-function. One must use a multiple-plane-wave representation. This leads to a very different expression for $\vec{v}(\vec{\mathbf{K}})$, and hence (2.5) is no longer the correct expression for $(\Delta\phi)^2$.

Before proceeding with the analysis, it should be noted that, thus far, no use has been made of the fact that we are discussing electron-dislocation scattering. Everything said so far applies equally well to electron-impurity scattering. The special feature of electron-dislocation scattering is that, for electron transport, very-small-angle scattering

events dominate $P_{\text{dis}}(\vec{\mathbf{K}}_1, \vec{\mathbf{K}}_2)$. Therefore, for electron-dislocation scattering, the final electron state $\vec{\mathbf{K}}_2$ always lies very close to the initial electron state $\vec{\mathbf{K}}_1$. In particular, if $\vec{\mathbf{K}}_1$ lies in the nonspherical portions of the Fermi surface, so will $\vec{\mathbf{K}}_2$. This implies that for $\vec{\mathbf{K}}_1$ in the nonspherical portions of the Fermi surface, one needs to use a multiple-plane-wave pseudo-wave-function for *both* $\vec{\mathbf{K}}_1$ and $\vec{\mathbf{K}}_2$. In practice, the two-plane-wave expression generally suffices. The importance of this result lies in the fact that for a two-plane-wave (2-PW) pseudo-wave-function for both $\vec{\mathbf{K}}_1$ and $\vec{\mathbf{K}}_2$ near the Brillouin-zone boundaries, one obtains

$$(\Delta\phi)_{2\text{-PW}}^2 \simeq \frac{1}{3} (e\hbar\tau_0/m)^2 [\hbar^2 G^2 / 4m |w(G)|]^2 q^2, \quad (2.6)$$

where $w(G)$ is the screened, electron-ion pseudopotential matrix element for the reciprocal-lattice vector \vec{G} which connects the two plane waves. The proof of this important result is presented in the Appendix. Equations (2.5) and (2.6) differ by the factor $[\hbar^2 G^2 / 4m |w(G)|]^2$. This factor is extremely large, being of order $10^2 - 10^3$ for the noble and polyvalent metals. In fact, because of the enormous enhancement of $(\Delta\phi)^2$ in the nonspherical portions of the Fermi surface, evaluation of (2.2) for ρ_{dis} with a constant $\tau_{\text{dis}}(\vec{\mathbf{K}})$ shows that the nonspherical portions dominate the integral for ρ_{dis} .

The situation is entirely different for electron-impurity scattering because large-angle scattering dominates ρ_{imp} . Here, "large-angle" scattering means that the scattering angle is larger than about 10° . For such scattering angles, it is extremely unlikely that both the initial and the final electron states will be in the nonspherical portions of the Fermi surface. Even if the initial state $\vec{\mathbf{K}}_1$ does lie in a nonspherical region, the final state $\vec{\mathbf{K}}_2$ will almost always lie in a spherical region. For such a case, (2.6) does not apply and there is no special enhancement of $(\Delta\phi)^2$ over (2.5). This is the basic reason why electron-dislocation scattering leads to such a different result for $\tau(\vec{\mathbf{K}})$ than does electron-impurity scattering.

Having seen the results of the calculation for ρ_{dis} based on $\tau_{\text{dis}}(\vec{\mathbf{K}}) = \tau_0$, we may readily choose a different functional form for $\tau_{\text{dis}}(\vec{\mathbf{K}})$ that will significantly reduce the value of ρ_{dis} . We simply eliminate the large contribution to ρ_{dis} resulting from the nonspherical portions of the Fermi surface by choosing a form for $\tau_{\text{dis}}(\vec{\mathbf{K}})$ that vanishes in these portions. Qualitatively, the functional form of $\tau_{\text{dis}}(\vec{\mathbf{K}})$ must have the following features:

$$\tau_{\text{dis}}(\vec{\mathbf{K}}) \simeq \begin{cases} \tau_0 & \vec{\mathbf{K}} \text{ in spherical portion,} \\ 0 & \vec{\mathbf{K}} \text{ in nonspherical portion.} \end{cases} \quad (27)$$

Such a form for $\tau_{\text{dis}}(\vec{\mathbf{K}})$ will drastically reduce the numerator of ρ_{dis} by about an order of magnitude. However, (2.7) will have but little effect on the denominator of ρ_{dis} , given by (2.2), because most of the Fermi surface of the noble and polyvalent metals is very nearly spherical and because the factor $(\Delta\phi)^2$ does not appear in the denominator.

The above discussion for the $\vec{\mathbf{K}}$ dependence of $\tau_{\text{dis}}(\vec{\mathbf{K}})$ also applies qualitatively to the relaxation time for electron-phonon scattering $\tau_{\text{ph}}(\vec{\mathbf{K}})$ for the polyvalent and noble metals. Indeed, the qualitative similarity between $\tau_{\text{dis}}(\vec{\mathbf{K}})$ and $\tau_{\text{ph}}(\vec{\mathbf{K}})$ for these metals was originally pointed out by Dugdale and Basinski¹³ and elaborated upon by Rowlands and Woods.⁷ We here calculate $\tau_{\text{dis}}(\vec{\mathbf{K}})$ explicitly and shall compare our results quantitatively with those we had previously obtained^{20,21,23} for $\tau_{\text{ph}}(\vec{\mathbf{K}})$. We find that, in spite of the qualitative similarity, there are important quantitative differences between $\tau_{\text{dis}}(\vec{\mathbf{K}})$ and $\tau_{\text{ph}}(\vec{\mathbf{K}})$, as we have previously¹⁵ pointed out.

A simple physical interpretation can be given for the form (2.7) for $\tau_{\text{dis}}(\vec{\mathbf{K}})$. The factor $(\Delta\phi)^2$ of (2.3) can be viewed as giving the “effectiveness” of a scattering event. In (2.2), one sees the well-known result¹⁷ that the contribution of a scattering event to ρ_{dis} depends not only on the probability that the scattering occurs, given by $P_{\text{dis}}(\vec{\mathbf{K}}_1, \vec{\mathbf{K}}_2)$, but also on the effectiveness of the scattering event in degrading the current, given by $(\Delta\phi)^2$. For electrons in the nonspherical portion of the Fermi surface, $(\Delta\phi)^2$ is so large for very-small-angle scattering, i.e., electron-dislocation scattering is so effective in degrading the current that these electrons are almost immediately scattered back to thermal equilibrium and thus removed from the current. In other words, the current does not contain any contribution from the electrons in the nonspherical portions of the Fermi surface. That is exactly the physical content of $\tau_{\text{dis}}(\vec{\mathbf{K}})$, as given in (2.7). A zero relaxation time means no contribution to the current.

A mathematical statement of the above result is contained in the variational theorem,¹⁷ which states that the exact $\tau_{\text{dis}}(\vec{\mathbf{K}})$ minimizes ρ_{dis} . Although (2.7) gives the general features of the $\vec{\mathbf{K}}$ dependence of $\tau_{\text{dis}}(\vec{\mathbf{K}})$ over the Fermi surface, a still better choice can be found by introducing into $\tau_{\text{dis}}(\vec{\mathbf{K}})$ a variational parameter. An effective way to do this

is to exploit the well-known fact¹⁷ that $v(\vec{\mathbf{K}})$ in the nonspherical portions of the Fermi surface is smaller than the Fermi velocity v_F . This suggests the form

$$\tau_{\text{dis}}(\vec{\mathbf{K}}) = \tau_0 [v(\vec{\mathbf{K}})/v_F]^n, \quad (2.8)$$

where the power n serves as a variational parameter. One includes v_F as a normalization factor so that for the spherical portions of the Fermi surface, the quantity in brackets equals unity. On the other hand, a large value for the power n will ensure that $\tau_{\text{dis}}(\vec{\mathbf{K}})$ nearly vanishes, as required, for $\vec{\mathbf{K}}$ in the nonspherical portions. The “best” choice for n for each metal is automatically provided by the variational theorem. One calculates ρ_{dis} as a function of n and finds the value of n that minimizes ρ_{dis} . This value gives the optimum choice for $\tau_{\text{dis}}(\vec{\mathbf{K}})$. We shall see that the optimum values are $n \simeq 7$ for Al and $n \simeq 1.5$ for the noble metals. The significant difference in the value of n for these two classes of metals can be understood in terms of the very different values of $|w(G)|$ and the different Fermi-surface topologies. Thus, the variational approach for determining $\tau_{\text{dis}}(\vec{\mathbf{K}})$ automatically takes into account these important features that distinguish Al from the noble metals by requiring different values for n for the two cases.

The functional form (2.8) that we propose for $\tau_{\text{dis}}(\vec{\mathbf{K}})$ is not new. We had previously introduced²⁰ this same functional form $\tau_{\text{ph}}(\vec{\mathbf{K}})$ and used it to calculate the low-temperature electron-phonon scattering resistivity for aluminum^{20,21} and for the noble metals.²³ This does not, of course, imply that the *degree* of anisotropy of $\tau_{\text{dis}}(\vec{\mathbf{K}})$ is the same as that of $\tau_{\text{ph}}(\vec{\mathbf{K}})$. The degree of anisotropy of the relaxation time is determined by the value of the exponent n . We shall see that for every metal considered, the calculated value of n appropriate to $\tau_{\text{dis}}(\vec{\mathbf{K}})$ is considerably smaller than that calculated^{21,23} for $\tau_{\text{ph}}(\vec{\mathbf{K}})$ at low temperatures. This shows that $\tau_{\text{ph}}(\vec{\mathbf{K}})$ at low temperatures is considerably more anisotropic over the Fermi surface than is $\tau_{\text{dis}}(\vec{\mathbf{K}})$.

III. OPTIMIZATION OF THE VARIATIONAL PARAMETER

Having chosen the parametrized form for $\tau_{\text{dis}}(\vec{\mathbf{K}})$, given in (2.8), we invoke the variational theorem¹⁷ to obtain the value of the power n that serves as a variational parameter. Thus, we calcu-

late ρ_{dis} as a function of n , to be denoted $\rho_{\text{dis}}(n)$, and find the value of n that minimizes $\rho_{\text{dis}}(n)$, to be denoted n_{min} . This is the value of n that is to be inserted into (2.8) for $\tau_{\text{dis}}(\vec{\mathbf{K}})$. The expression for $\rho_{\text{dis}}(n)$ is given in (2.2). To evaluate the integrals, one needs as input data the electronic properties of each metal and the expression for $P_{\text{dis}}(\vec{\mathbf{K}}_1, \vec{\mathbf{K}}_2)$.

The electronic properties of Al that we used in the present calculation are based on the piecewise two-orthogonalized-plane-wave (2-OPW) scheme.²¹ The central idea is that for each point $\vec{\mathbf{K}}$ on the Fermi surface, a linear combination of the two plane waves $|\vec{\mathbf{K}}\rangle$ and $|\vec{\mathbf{K}}-\vec{\mathbf{G}}\rangle$ is taken to calculate the pseudo-wave-functions and the Fermi surface. For each point $\vec{\mathbf{K}}$, one chooses the reciprocal-lattice vector $\vec{\mathbf{G}}$ that produces the greatest distortion of the Fermi surface from sphericity. This is clearly the most important $\vec{\mathbf{G}}$ for that particular point $\vec{\mathbf{K}}$. For the values of the screened pseudopotential matrix elements, $w(G)$, we used those deduced by Ashcroft²⁴ from his analysis of the de Haas—van Alphen data. For Al, both $w(G_{111})$ and $w(G_{200})$ must be included in the calculation. Complete details have been given by Kaveh and Wiser.²¹

For the noble metals, the Fermi surface was approximated by the 8-cone model of Ziman.²⁵ The central idea is that the free-electron sphere is replaced by the intersections of a sphere and the eight cones whose axes lie in the eight $\{111\}$ directions. One then computes the distortion of the Fermi surface from sphericity arising from the relatively large screened pseudopotential matrix element $w(G_{111})$. Unlike Al, for the noble metals, only $w(G_{111})$ need be included in the calculation of the Fermi surface and the pseudo-wave-functions. The magnitude of $w(G_{111})$ for the noble metals is so large that the Fermi surface makes contact with the Brillouin-zone boundaries at the hexagonal zone faces to form “necks.” The value of $w(G_{111})$ for each of the noble metals is given by the radius of the neck at the point of contact, as measured by the de Haas—van Alphen experiment. For the pseudo-wave-function, one uses a linear combination of two plane waves $|\vec{\mathbf{K}}\rangle$ and $|\vec{\mathbf{K}}-\vec{\mathbf{G}}\rangle$, where $\vec{\mathbf{G}}$ is the $[111]$ reciprocal-lattice vector appropriate to the cone associated with the point $\vec{\mathbf{K}}$ on the Fermi surface. Complete details have been given by Ziman.²⁵

For the electron-dislocation scattering transition probability $P_{\text{dis}}(\vec{\mathbf{K}}_1, \vec{\mathbf{K}}_2)$, we adopt a simple model which contains the salient physics. The principal dependence of $P_{\text{dis}}(\vec{\mathbf{K}}_1, \vec{\mathbf{K}}_2)$ on the electron states

$\vec{\mathbf{K}}_1$ and $\vec{\mathbf{K}}_2$ is through the scattering angle or, equivalently, through the magnitude of the momentum transfer $q = |\vec{\mathbf{K}}_1 - \vec{\mathbf{K}}_2|$. Thus, $P_{\text{dis}}(\vec{\mathbf{K}}_1, \vec{\mathbf{K}}_2) \rightarrow P_{\text{dis}}(q)$. The existence of a sharp peak in $P_{\text{dis}}(q)$ for very-small-angle scattering^{18,19} suggests the q dependence of $P_{\text{dis}}(q)$ can be sensibly replicated by a Gaussian of narrow width. Thus,

$$P_{\text{dis}}(q) \propto \left\{ \exp\left[-\frac{1}{2}(q/q_0)^2\right] \right\}, \quad (3.1)$$

where q_0 gives the half-width of the peak. The result for n_{min} , and hence for $\tau_{\text{dis}}(\vec{\mathbf{K}})$, was found not to be sensitive to the value assumed for q_0 providing its value is small enough to correspond to a scattering angle of less than 1° .

The form of $P_{\text{dis}}(q)$ given in (3.1) is appropriate only if one assumes that very-small-angle scattering events dominate electron-dislocation scattering. Therefore, it is in place to review the evidence supporting this assumption. A clear summary of the experimental evidence has been given by Chang and Higgins.¹⁸ Their main point is that the measured effective scattering rate for electron-dislocation scattering is about 30 times larger for the de Haas—van Alphen effect, which is sensitive to electron scattering through angles as small as $\sim 0.01^\circ$, than for the radio-frequency size effect, which is not sensitive to electron scattering unless the scattering angle exceeds $\sim 1^\circ$. It follows, therefore, that the angular dependence of the electron-dislocation scattering cross section must have a sharp peak that is very much narrower than 1° . In other words, these data imply that the electron-dislocation scattering rate must depend on the scattering angle in a way that is quite similar to that given by Eq. (3.1). Indeed, Fig. 17 of the paper by Chang and Higgins,¹⁸ in which an “experimental” curve for $P_{\text{dis}}(q)$ is plotted schematically as a function of q (scattering angle), might almost be a plot of our Eq. (3.1).

The theoretical basis for the dominance of very-small-angle electron-dislocation scattering events has been provided by several recent calculations.¹⁹ However, it is clear from these calculations that the problem of electron-dislocation scattering is rather complex, and has in fact been the subject of controversy. The consensus that seems to be emerging^{18,19} is that very-small-angle scattering events are certainly very important and probably even dominate the electron-dislocation scattering rate. This is the view that we adopt here.

The form of $P_{\text{dis}}(q)$ given in (3.1) assumes isotropic scattering and thus ignores the fact that a dislocation line is an anisotropic scattering center.

It should be emphasized that even an isotropic scattering center will yield an anisotropic relaxation time $\tau(\vec{K})$ because of the anisotropy arising from the nonsphericity of the Fermi surface. It is our thesis that Fermi-surface nonsphericity is the major source of anisotropy of $\tau_{\text{dis}}(\vec{K})$ for the polyvalent and noble metals.

One need not ignore altogether the anisotropy of the dislocation lines. This anisotropy may be simulated in various ways. For example, we can restrict $P_{\text{dis}}(\vec{K}_1, \vec{K}_2)$ to scattering events for which the vector momentum transfer \vec{q} lies within a given angle θ of the reciprocal-lattice vector \vec{G} that enters the pseudo-wave-function of the electron states \vec{K}_1 and \vec{K}_2 . (Since only small-angle scattering is possible, the same \vec{G} is always relevant to both \vec{K}_1 and \vec{K}_2 .) We calculated n_{min} for a series of values of θ ranging from $\theta=90^\circ$ (no restriction at all, i.e., all scattering events included) to $\theta=50^\circ$ (only $\sim 35\%$ of the scattering events included). Both for the noble metals and for Al, we found that assuming that the dislocation line is a completely isotropic scattering center ($\theta=90^\circ$) yielded a value of n_{min} quite similar to that obtained upon introducing a rather severe anisotropy ($\theta=50^\circ$) for electron-dislocation scattering. This relative insensitivity of n_{min} of the value assumed for θ supports our contention that the principal source of anisotropy in $\tau_{\text{dis}}(\vec{K})$ arises from the anisotropy of the Fermi surface, rather than from the anisotropy of the electron-dislocation scattering.

We calculated n_{min} both as a function of q_0 and as a function of θ . There is, of course, no reason to restrict n_{min} to integral values. In Fig. 1, the results for n_{min} are presented for Ag for several values of q_0 . Following Ziman,²⁵ we measure q_0 in units of $\frac{1}{2}G_{111}$, the distance ΓL from the center of the Brillouin zone to the midpoint of a hexagonal face. In these units, a little geometry shows that a maximum scattering angle of 1° corresponds to $q_0 \approx 0.013$. Thus, the values of q_0 plotted in Fig. 1 correspond to maximum scattering angles ranging from $\frac{1}{4}^\circ$ to $\frac{3}{4}^\circ$. The resulting values for n_{min} vary from 1.3 to 2.4. In Fig. 2, we present the results for n_{min} for the other noble metals as a function of $\cos\theta$ for $q_0=0.003$. Once again, the variation of n_{min} with $\cos\theta$ is not severe. For Cu, we find that n_{min} ranges from 1.4 to 2.1; for Au, the variation of n_{min} is from 1.2 to 1.7. It is unlikely that there is any significance to these slight differences in the ranges of n_{min} found between one noble metal and another, in view of the simplicity of our model for $P_{\text{dis}}(\vec{K}_1, \vec{K}_2)$.

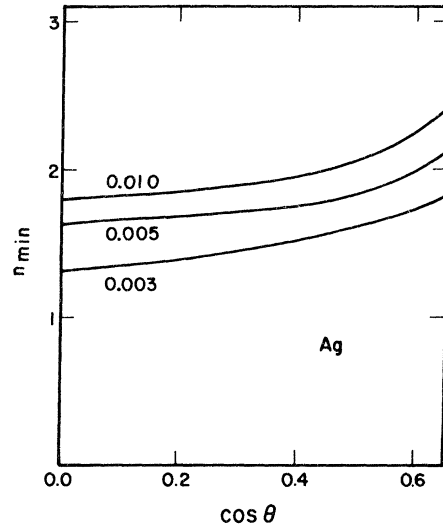


FIG. 1. Calculated values of n_{min} for Ag as a function of $\cos\theta$ for several different values of q_0 .

The calculated results for Al are presented in Fig. 3 as a function of $\cos\theta$ for two values of q_0 . Once again, one sees that the dependence of n_{min} on q_0 is weaker than the dependence on $\cos\theta$. The variation of n_{min} is from ~ 6 to ~ 8 . The much larger value of n_{min} for Al, as compared to the noble metals, is due to the much smaller value for $w(G_{111})$ for Al and to the fact that the Fermi surface of Al is not confined to the first Brillouin zone.

The results for all the metals studied may be

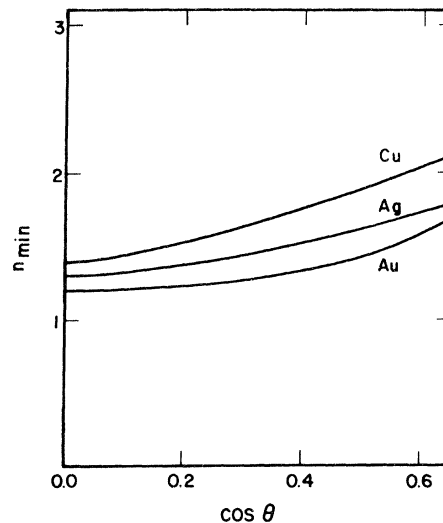


FIG. 2. Calculated values of n_{min} for the noble metals as a function of $\cos\theta$ for $q_0=0.003$.

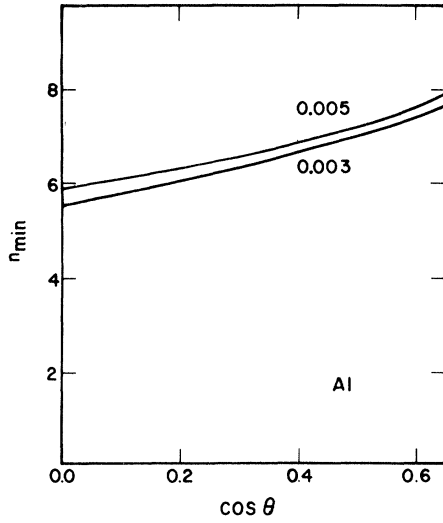


FIG. 3. Calculated values of n_{\min} for Al as a function of $\cos\theta$ for two different values of q_0 .

summarized as follows:

$$n_{\min} \simeq \begin{cases} 1.5 \pm 0.5 & \text{for the noble metals} \\ 7 \pm 1 & \text{for Al.} \end{cases} \quad (3.2)$$

It is instructive to compare these values for n_{\min} for electron-dislocation scattering with the corresponding values for electron-phonon scattering at low temperatures. We have already mentioned that the functional form (2.8) for the relaxation time is also appropriate to describe the low-temperature electron-phonon scattering relaxation time $\tau_{\text{ph}}(\vec{K})$ for Al and the noble metals. However, because of the properties of the electron-phonon scattering transition probability, the \vec{K} dependence of $\tau_{\text{ph}}(\vec{K})$ is much more pronounced than for $\tau_{\text{dis}}(\vec{K})$. This implies a much larger value for the power n , as is confirmed by the explicit calculations. The calculation of $\tau_{\text{ph}}(\vec{K})$ yields that for aluminum,²¹ n_{\min} varies from 50 at about 20 K to 10 at about 50 K, whereas for silver,²³ n_{\min} varies from 10 at about 5 K to 6 at about 20 K. The values of n_{\min} for $\tau_{\text{ph}}(\vec{K})$ are higher for Al than for Ag for essentially the same reasons as given above for $\tau_{\text{dis}}(\vec{K})$.

Another quantity of interest is the magnitude of the reduction in $\rho_{\text{dis}}(n)$ upon using $\tau_{\text{dis}}(\vec{K})$, given by $n = n_{\min}$, rather than using the simple relaxation-time approximation of a constant τ_0 , given by setting $n = 0$ in (2.8). In other words, we consider the magnitude of the ratio $\rho_{\text{dis}}(0)/\rho_{\text{dis}}(n_{\min})$. Unlike the situation for n_{\min} , the value of this ratio depends significantly on the value assumed for θ . The calculated results are

$$\frac{\rho_{\text{dis}}(0)}{\rho_{\text{dis}}(n_{\min})} \simeq \begin{cases} 10 & \text{for the noble metals} \\ 5 & \text{for Al} \end{cases} \quad (3.3)$$

with a factor-of-2 uncertainty in the above values due to their variation with θ . It is not unexpected to find that the calculated values of the ratio $\rho_{\text{dis}}(0)/\rho_{\text{dis}}(n_{\min})$ have a much greater uncertainty than the calculated values of n_{\min} , because $\rho_{\text{dis}}(n)$ is much more sensitive to the details of $P_{\text{dis}}(\vec{K}_1, \vec{K}_2)$ than is $\tau_{\text{dis}}(\vec{K})$.

IV. REAL SAMPLES

Thus far, the discussion has been limited to samples for which one may ignore the contribution to the residual resistivity due to electron-impurity scattering ρ_{imp} , i.e., $\rho_{\text{dis}} \gg \rho_{\text{imp}}$. For a real sample, of course, this is rarely the case. Therefore, we shall generalize the analysis to make it appropriate to samples having an arbitrary value of the ratio $\rho_{\text{dis}}/\rho_{\text{imp}}$. The expression for ρ_{imp} is given by Eq. (2.2) with $\rho_{\text{dis}}(\vec{K}_1, \vec{K}_2)$ replaced by the transition probability for electron-impurity scattering $P_{\text{imp}}(\vec{K}_1, \vec{K}_2)$. For $\phi(\vec{K})$, we insert the expression given by Eq. (2.1) with $\tau_{\text{dis}}(\vec{K})$ replaced by the electron-impurity scattering relaxation time $\tau_{\text{imp}}(\vec{K})$.

The determination of $\tau_{\text{imp}}(\vec{K})$ is simple because one may use the relaxation-time approximation of a constant $\tau_{\text{imp}}(\vec{K})$. It has been shown²⁶ that this approximation yields very accurate values of ρ_{imp} , in spite of the fact that the relaxation-time approximation is not exact even for a spherical scattering center because of the nonsphericity of the Fermi surface of the polyvalent and noble metals. Sorbello²⁶ has calculated ρ_{imp} by iterating the Boltzmann equation to convergence and found that the results are within a few percent of the values obtained from simply assuming $\tau_{\text{imp}}(\vec{K}) = \text{const}$. Moreover, this result was found to apply to a wide variety of impurity atoms. This confirms the well-known result¹⁷ that $\tau_{\text{imp}}(\vec{K})$ is insensitive to the details of $P_{\text{imp}}(\vec{K}_1, \vec{K}_2)$.

We may exploit this insensitivity by using the simple model of Eq. (3.1) for $P_{\text{imp}}(\vec{K}_1, \vec{K}_2)$ with the magnitude of q_0 being $\geq k_F$ to take account of the fact that large-angle scattering is important for ρ_{imp} . In fact, we find that there is no significant difference between assuming $q_0 \simeq k_F$ and assuming $q_0 \rightarrow \infty$. For the present discussion of electron-impurity scattering, the only requirement is that the magnitude of q_0 be sufficiently large to permit

scattering events for which the scattering angle is larger than about 10° .

The functional form given in Eq. (2.8) to describe $\tau_{\text{dis}}(\vec{K})$ can also be used to describe $\tau_{\text{imp}}(\vec{K})$ if one sets $n=0$. This suggests introducing the notation $n_{\text{imp}}(=0)$ for the value of n that minimizes $\rho_{\text{imp}}(n)$ and the notation n_{dis} (previously denoted n_{min}) for the value of n that minimizes $\rho_{\text{dis}}(n)$. This notation permits us to describe the \vec{K} dependence of the relaxation time of a real sample (RS) within the same framework of Eq. (2.8). Thus, we write:

$$\tau_{\text{RS}}(\vec{K}) = \tau_0 [v(\vec{K})/v_F]^n. \quad (4.1)$$

The value of n appropriate to $\tau_{\text{RS}}(\vec{K})$ for a real sample, characterized by a given value of the ratio $\rho_{\text{dis}}/\rho_{\text{imp}}$, is determined by the variational theorem. One writes the total residual resistivity as a function of the variational parameter n :

$$\rho_0(n) = \rho_{\text{dis}}(n) + \rho_{\text{imp}}(n). \quad (4.2)$$

For a given value of the ratio $\rho_{\text{dis}}/\rho_{\text{imp}}$, one calculates the value of n (to be denoted n_{RS}) that minimizes $\rho_0(n)$. The limiting cases are clear. For a sample for which $\rho_{\text{imp}} \gg \rho_{\text{dis}}$, one has $n_{\text{RS}} \simeq n_{\text{imp}} = 0$ and $\tau_{\text{RS}}(\vec{K}) \simeq \tau_{\text{imp}}(\vec{K}) = \tau_0$. On the other hand, for a sample for which $\rho_{\text{dis}} \gg \rho_{\text{imp}}$, one has $n_{\text{RS}} \simeq n_{\text{dis}} (\simeq 1.5$ for the noble metals and $\simeq 7$ for Al) and $\tau_{\text{RS}}(\vec{K}) \simeq \tau_{\text{dis}}(\vec{K})$. For the general case, for which ρ_{imp} and ρ_{dis} are the same order of magnitude, one has:

$$n_{\text{imp}} < n_{\text{RS}} < n_{\text{dis}}, \quad (4.3)$$

with the value of n_{RS} being determined by the outcome of the "competition" for any given sample between the dislocations and the impurities for the role of dominant electron scatterer.

The explicit determination of n_{RS} requires calculating the n dependence of both $\rho_{\text{imp}}(n)$ and $\rho_{\text{dis}}(n)$. We have already discussed in Sec. III the calculation of the n dependence of $\rho_{\text{dis}}(n)$. Our results were summarized in Eq. (3.3), where it is seen that $\rho_{\text{dis}}(n)$ increases by about an order of magnitude as n decreases from n_{dis} to $n_{\text{imp}}=0$. The results of calculation of the n dependence of $\rho_{\text{imp}}(n)$ can be summarized as follows:

$$\frac{\rho_{\text{imp}}(n_{\text{dis}})}{\rho_{\text{imp}}(0)} \simeq \begin{cases} 1.3 & \text{for the noble metals} \\ 1.4 & \text{for Al.} \end{cases} \quad (4.4)$$

Note the dramatic contrast between the results of (3.3) for $\rho_{\text{dis}}(n)$ and of (4.4) for $\rho_{\text{imp}}(n)$. The use of $\tau_{\text{imp}}(\vec{K})$ to calculate ρ_{dis} increases the resistivity in-

tegral by as much as an order of magnitude, whereas the use of $\tau_{\text{dis}}(\vec{K})$ to calculate ρ_{imp} increases the resistivity integral by only 30–40%. This illustrates once again the fact that the calculated value of ρ_{imp} is relatively insensitive to the \vec{K} dependence of the relaxation time.

Having calculated the n dependence of both $\rho_{\text{dis}}(n)$ and $\rho_{\text{imp}}(n)$, and hence of $\rho_0(n)$, we can obtain the value of n_{RS} for any given value of the ratio $\rho_{\text{dis}}/\rho_{\text{imp}}$. It should be noted that the value of the ratio $\rho_{\text{dis}}/\rho_{\text{imp}}$ refers to its value for $n=n_{\text{RS}}$. Our results for Al are given in Fig. 4, where we plot n_{RS} as a function of $\rho_{\text{dis}}/\rho_{\text{imp}}$. The curve gives the calculated results; the circles are "experimental" points which will be discussed presently. The calculation of $\rho_{\text{dis}}(n)$ was based on the values $q_0=0.003$ and $\theta=90^\circ$ for $P_{\text{dis}}(q)$. As indicated in Eq. (3.2), the dependence of the results on q_0 and on θ implies an uncertainty of ~ 1 in the calculated value of n_{RS} .

We now turn to the circles in Fig. 4, which constitute a sort of "experimental" test of our theory. The "experimental" points, which were taken²⁷ from Fig. 7 of Ref. 12, were obtained as follows. For a sample of Al with a given value of $\rho_{\text{dis}}/\rho_{\text{imp}}$, the relaxation time $\tau_{\text{RS}}(\vec{K})$ determines not only the calculated residual resistivity ρ_0 but also the calculated temperature-dependent term of the resistivity $\Delta\rho(T)$. The magnitude of $\Delta\rho(T)$ at low temperatures is so small compared with ρ_0 that $\Delta\rho(T)$ does not affect the relaxation time. Low-temperature calculations^{12,15} of $\Delta\rho(T)$ based on $\tau_{\text{RS}}(\vec{K})$ have recently been carried out for Al and compared with

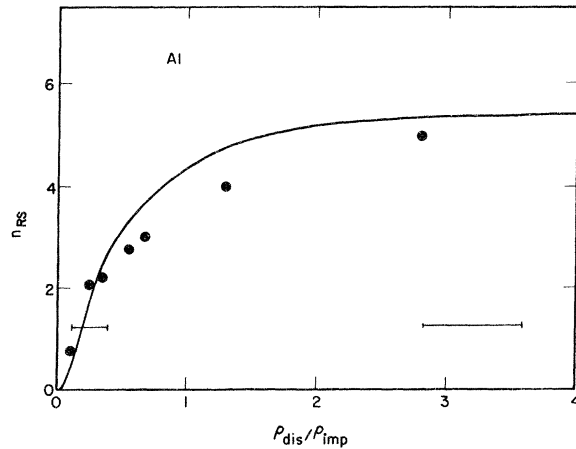


FIG. 4. Calculated values of n_{RS} for Al as a function of the ratio $\rho_{\text{dis}}/\rho_{\text{imp}}$. The circles are the values previously deduced by empirical means from the low-temperature $\Delta\rho(T)$ data (see Ref. 12).

experimental results, both for cold-worked samples⁷ and for annealed samples.¹² It should be emphasized that the calculation of $\Delta\rho(T)$ contains no adjustable parameters,²¹ other than n_{RS} . The value of n_{RS} was determined empirically, i.e., n_{RS} was an empirical parameter in the calculation whose value was chosen for each sample to give the best overall fit between the calculated and the measured results for $\Delta\rho(T)$ for the sample. This procedure yields a value for n_{RS} that is accurate to within 0.2.

The value for the ratio ρ_{dis}/ρ_{imp} for each sample was determined in the following way. For the cold-worked samples,⁷ the value of ρ_{dis}/ρ_{imp} was obtained by assuming that for the initial unstrained annealed sample, ρ_{dis} is negligible and ρ_{imp} equals the measured residual resistivity ρ_0 . Subsequent cold-working increases ρ_{dis} without affecting ρ_{imp} . Thus, the increase in the measured ρ_0 upon cold-working is ascribed to an increase in ρ_{dis} . For the annealed samples,¹² the ratio ρ_{dis}/ρ_{imp} was taken to be $\sim \frac{1}{4}$ for the sample that was annealed for 2 h at 270°C (see Ref. 12 for justification). This fixes ρ_{imp} for all the samples. Since annealing reduces ρ_{dis} without affecting ρ_{imp} , the measured reduction in ρ_0 upon annealing is ascribed to a reduction in ρ_{dis} .

We now estimate the uncertainty in the resulting value of ρ_{dis}/ρ_{imp} . Let us assume for the cold-worked samples⁷ that even in the annealed unstrained state, up to 20% of ρ_0 may be due to ρ_{dis} , thus introducing an uncertainty of 20% into the value of ρ_{imp} . Similarly, let us assume for the annealed samples¹² that the value of ρ_{imp} is uncertain by up to 20%. These assumptions lead to the uncertainties in the values of the ratio ρ_{dis}/ρ_{imp} that are indicated by the horizontal bars in Fig. 4. Since the uncertainty varies with the value of ρ_{dis}/ρ_{imp} , we have included two horizontal bars in two different regions of the figure.

In summary, we may use the data for $\Delta\rho(T)$ on cold-worked⁷ and annealed¹² samples of Al to deduce values of n_{RS} as a function of ρ_{dis}/ρ_{imp} . The results may be regarded almost as “experimental” data points, which are plotted as circles in Fig. 4. The agreement between the calculated curve for n_{RS} -vs- ρ_{dis}/ρ_{imp} and the “experimental” data points is evident from the figure.

The calculated results for the noble metals are presented in Fig. 5, where we plot n_{RS} as a function the ratio ρ_{dis}/ρ_{imp} for Cu, Ag, and Au. The calculations were based on the values $q_0=0.003$ and $\cos\theta=0.6$. As indicated in Eq. (3.2), the uncertainty in the calculated values of n_{RS} is ~ 0.5

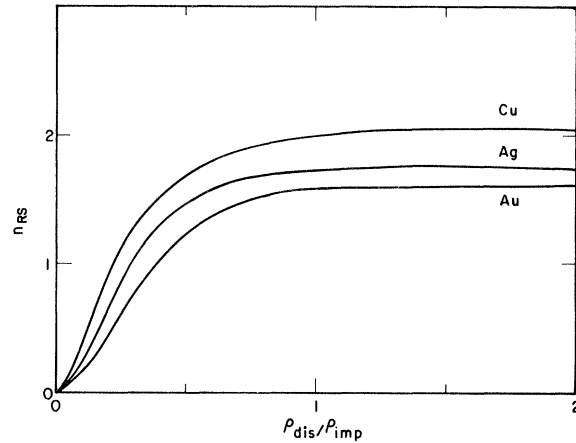


FIG. 5. Calculated values of n_{RS} for the noble metals as a function of the ratio ρ_{dis}/ρ_{imp} .

due to the dependence of the results on the values chosen for q_0 and θ .

Although we have not included any “experimental” data points in Fig. 5, as we did in Fig. 4 for Al, there does exist evidence regarding Ag that supports the magnitude of the calculated values for n_{RS} given in Fig. 5. The same procedure that led to the “experimental” data points for Al of Fig. 4 was also used^{14,15} to calculate $\Delta\rho(T)$ for Ag. It was found that empirical values of ~ 1 for n_{RS} led to good agreement between the theory^{14,15} and experiment^{6,9} for $\Delta\rho(T)$ for the unstrained samples of Ag that were measured, in agreement with the calculated curve of Fig. 5. However, we cannot include these “experimental” results in Fig. 5 because there is no clear method for determining the value of ρ_{dis}/ρ_{imp} for these samples. Nevertheless, the empirical values of n_{RS} for these samples of Ag is certainly about what one would expect from the calculated curve of Fig. 5. Moreover, we note that the large difference in the values of n_{RS} for Al as compared to Ag that results from the theory (compare Figs. 4 and 5) is reproduced in the empirical values of n_{RS} that are deduced for these two metals from the low-temperature calculations of $\Delta\rho(T)$. This close correlation between theory and “experiment” for the different metals certainly seems to be significant.

V. ELECTRON-PHONON SCATTERING AND ELECTRON-ELECTRON SCATTERING

We now discuss some of the implications of the present analysis of $\tau_{dis}(\vec{K})$. Of particular interest is

the effect of $\tau_{\text{dis}}(\vec{\mathbf{K}})$ on the sample dependence of the low-temperature electron-phonon scattering contribution $\rho_{\text{ph}}(T)$ and the electron-electron scattering contribution $\rho_{\text{el}}(T)$ to the electrical resistivity. At low temperatures, all samples correspond to the "dirty limit," by which one means that the residual resistivity ρ_0 dominates the other scattering process, $\rho_0 \gg \rho_{\text{ph}}(T) + \rho_{\text{el}}(T)$. Therefore, the appropriate relaxation time is given by $\tau_{\text{RS}}(\vec{\mathbf{K}})$ of Eq. (4.1), with the value of the exponent n_{RS} being determined by the value of the ratio $\rho_{\text{dis}}/\rho_{\text{imp}}$ characterizing the particular sample under consideration. The essential point is that in the dirty limit, $\tau_{\text{RS}}(\vec{\mathbf{K}})$ is the relaxation time that determines *all* scattering processes, including both $\rho_{\text{ph}}(T)$ and $\rho_{\text{el}}(T)$. Hence, the values of both $\rho_{\text{ph}}(T)$ and $\rho_{\text{el}}(T)$ depend on n_{RS} , which in turn depends on the ratio $\rho_{\text{dis}}/\rho_{\text{imp}}$ for the sample. For this reason, two samples with different values of $\rho_{\text{dis}}/\rho_{\text{imp}}$ will have different values for $\rho_{\text{ph}}(T)$ and for $\rho_{\text{el}}(T)$, even though both samples may have the same residual resistivity.

The calculation of the sample dependence of $\rho_{\text{ph}}(T)$ and $\rho_{\text{el}}(T)$, based on Eq. (4.1) for $\tau_{\text{RS}}(\vec{\mathbf{K}})$, has recently been carried out.^{12,14-16,23} The most interesting result of the calculation is that the effect of straining the samples, and thus increasing $\rho_{\text{dis}}/\rho_{\text{imp}}$, leads to *opposite* effects for $\rho_{\text{ph}}(T)$ and for $\rho_{\text{el}}(T)$. An increase in $\rho_{\text{dis}}/\rho_{\text{imp}}$ *decreases* (Ref. 15) $\rho_{\text{ph}}(T)$ but *increases* $\rho_{\text{el}}(T)$. Of course, annealing the samples reverses the effects, increasing $\rho_{\text{ph}}(T)$ while decreasing $\rho_{\text{el}}(T)$.

These results can be understood qualitatively in the following way. We first discuss $\rho_{\text{ph}}(T)$. If one considers a sample without dislocations, then $\rho_{\text{dis}}=0$, $\rho_0=\rho_{\text{imp}}$, and one has the usual deviations from Matthiessen's rule.¹ The essence of this phenomenon is that, at a fixed temperature, the value of $\rho_{\text{ph}}(T)$ is larger for samples having larger values of ρ_0 . The explanation²⁰ for this phenomenon is that in the pure limit [$\rho_0 \ll \rho_{\text{ph}}(T)$], the appropriate relaxation time is $\tau_{\text{ph}}(\vec{\mathbf{K}})$, whereas in the dirty limit [$\rho_0 \gg \rho_{\text{ph}}(T)$], the appropriate relaxation time is $\tau_{\text{imp}}(\vec{\mathbf{K}})$. The sample dependence of $\rho_{\text{ph}}(T)$ at a fixed temperature arises solely from the change in relaxation time. The calculation^{20,21} shows that at low temperatures, the relaxation time $\tau_{\text{imp}}(\vec{\mathbf{K}})$ yields a value of $\rho_{\text{ph}}(T)$ that is very much larger than that obtained with the relaxation time $\tau_{\text{ph}}(\vec{\mathbf{K}})$, in complete agreement with experiment.¹

Now consider samples that contain a significant density of dislocations. For such samples, the appropriate relaxation time is $\tau_{\text{RS}}(\vec{\mathbf{K}})$, given by Eq.

(4.1). Moreover, as the ratio $\rho_{\text{dis}}/\rho_{\text{imp}}$ increases, the relaxation time approaches $\tau_{\text{dis}}(\vec{\mathbf{K}})$. But, as we have already remarked, $\tau_{\text{dis}}(\vec{\mathbf{K}})$ resembles $\tau_{\text{ph}}(\vec{\mathbf{K}})$ qualitatively, although with a much smaller value of the exponent n . In other words, the effect of increasing the dislocation density of the sample, and thus increasing $\rho_{\text{dis}}/\rho_{\text{imp}}$, is to make the relaxation time resemble $\tau_{\text{ph}}(\vec{\mathbf{K}})$ more closely. Thus, straining the sample has the same effect as partially driving the sample toward the pure limit, with a corresponding decrease in the value of $\rho_{\text{ph}}(T)$.

These ideas have served as the basis for explicit calculations of the effect of dislocations on $\rho_{\text{ph}}(T)$ at low temperatures for polyvalent and noble metals. For Al, the calculations^{12,15} have explained quantitatively the observed⁷ decrease in $\rho_{\text{ph}}(T)$ upon cold-working the samples and the observed¹² increase in $\rho_{\text{ph}}(T)$ upon annealing the samples. For Ag, the calculations^{14,15,23} have explained quantitatively the marked sample dependence observed^{6,9} for $\rho_{\text{ph}}(T)$ for samples having almost the same value of ρ_0 .

We now discuss the effect of electron-dislocation scattering on $\rho_{\text{el}}(T)$. First, consider a sample without dislocations. Then, $\rho_{\text{dis}}=0$, $\rho_0=\rho_{\text{imp}}$, and $\tau(\vec{\mathbf{K}})=\tau_{\text{imp}}(\vec{\mathbf{K}})=\text{const}$ is the appropriate relaxation time. As discussed earlier, this is the case even though the Fermi surface of the polyvalent and noble metals is not spherical. It is sufficient that most of the Fermi surface be very nearly spherical. For electron-impurity scattering, nothing special happens because of the small regions of nonsphericity of the Fermi surface near the Brillouin-zone boundaries, and these regions therefore have no effect on the determination of $\tau_{\text{imp}}(\vec{\mathbf{K}})$. A very similar situation prevails for electron-electron scattering. Here, too, nothing special happens because of the small deviations of the Fermi surface from sphericity. Therefore, a spherical Fermi surface and the one-orthogonalized-plane-wave (1-OPW) approximation to the electron wave functions constitutes a reasonable first approximation. Before exploring the consequences of this approximation, we emphasize that this approximation is totally invalid for discussing electron-dislocation scattering or electron-phonon scattering, for which the small deviations of the Fermi surface from sphericity are of crucial importance.

For an isotropic ($\vec{\mathbf{K}}$ independent) relaxation time and 1-OPW wave functions, it is well known¹⁷ that normal electron-electron scattering does not contribute to the resistivity. A normal electron-electron scattering event merely involves an exchange of

momentum between the two electrons being scattered, without any net momentum loss to the system and hence is not a resistive scattering process. Moreover, for a 1-OPW electron wave function, umklapp electron-electron scattering events do not occur because of translational invariance.¹⁷ Therefore, $\rho_{el}(T)$ vanishes. Only when the multiple-OPW character of the wave function is taken into account does one obtain a nonzero $\rho_{el}(T)$.

A recent analysis¹⁶ has shown that this situation is fundamentally changed when the relaxation time is not isotropic, but rather depends on \vec{K} , as occurs in the presence of electron-dislocation scattering. Then, even for 1-OPW wave functions, normal electron-electron scattering events *do* increase the resistivity by scattering the electrons into regions of the Fermi surface of strong scattering. The increased resistivity implies a nonzero $\rho_{el}(T)$ even for 1-OPW wave functions. Therefore, the presence of dislocations increases the total $\rho_{el}(T)$ by adding a normal-scattering 1-OPW contribution to the usual umklapp-scattering multiple-OPW contribution that is always present, even in the absence of electron-dislocation scattering.

Although a quantitative calculation of the enhancement of $\rho_{el}(T)$ due to electron-dislocation scattering has not been carried out for noble and polyvalent metals, it is not difficult to estimate the magnitude of the effect. From the calculations^{28–30} of the anisotropy factor Δ for polyvalent and noble metals, it follows that the umklapp term is roughly half as large as the maximum value of the normal term. Thus, the maximum possible normal contribution would enhance $\rho_{el}(T)$ by roughly a factor of 3 over its umklapp value. Since the anisotropy of the dislocation relaxation time enhances the normal contribution to about 10% of its maximum value,¹⁶ we should expect that $\rho_{el}(T)$ would be enhanced by about 30%, with something like a factor-of-2 uncertainty in the value. In other words, the magnitude of $\rho_{el}(T)$ for a sample containing primarily dislocations with few impurities should be about 20–60% larger than for a sample containing primarily impurities with few dislocations.

We now consider the experimental evidence for this predicted enhancement of $\rho_{el}(T)$ for polyvalent and noble metals. There are recent, accurate low-temperature resistivity data available for Al and for Ag. For Al, the data of Ribot *et al.*¹³ exhibit a sample dependence of $\sim 0–15\%$ for $\rho_{el}(T)$, whereas the data of Sinvani *et al.*¹² exhibit a sample dependence of $\sim 20–30\%$ for $\rho_{el}(T)$. For Ag,

the analysis¹⁴ of the various recent data^{6,9,32} show about a 50% enhancement in $\rho_{el}(T)$ for samples with a larger value of ρ_{dis}/ρ_{imp} . These results are certainly consistent with the above estimate of the enhancement factor of $\rho_{el}(T)$ due to electron-dislocation scattering. Moreover, note that the enhancement factor of Ag is clearly larger than for Al. Other quantitative differences between Al and Ag have previously been noted in this paper.

Finally, a few words should be said about the alkali metals. Although the calculation of $\tau_{dis}(\vec{K})$ for the alkali metals does not lie within the scope of this paper, it is nevertheless in place to point out that the results for the alkali metals are very different from those of the polyvalent and noble metals with regard to both $\rho_{ph}(T)$ and $\rho_{el}(T)$. First, the enhancement of $\rho_{el}(T)$ due to electron-dislocation scattering is very much larger for the alkali metals than for the polyvalent or noble metals. This difference is due to the fact that the alkali-metal wave functions are primarily 1-OPW in character. This fact explains the order-of-magnitude enhancement factor for $\rho_{el}(T)$ observed for \vec{K} in recent experiments.^{16,33} It also explains the anomalously large value for $\rho_{el}(T)$ recently observed³⁴ for Li. Second, the effect of electron-dislocation scattering on $\rho_{ph}(T)$ is to *increase* $\rho_{ph}(T)$ for the alkali metals,³⁵ in direct contrast to the situation for the polyvalent and noble metals. The reason for this totally different behavior for $\rho_{ph}(T)$ for these two classes of metals is due to the phenomenon of phonon drag.¹⁷ Phonon drag is an important effect for $\rho_{ph}(T)$ *only* for the alkali metals, but *not* for the polyvalent and noble metals.³⁶ A complete discussion of these various ideas will be presented in separate publications.

VI. SUMMARY

A calculation has been performed of the relaxation time for electron-dislocation scattering for polyvalent and noble metals, based on a simple model for the transition probability for electron-dislocation scattering. Our principal results are the following.

(i) The marked \vec{K} dependence of $\tau_{dis}(\vec{K})$ for polyvalent and noble metals was shown to arise from a combination of two factors, viz., the nonsphericity of the Fermi surface and the predominance of very-small-angle scattering events for electron-dislocation scattering.

(ii) A large quantitative difference was found be-

tween the $\tau_{\text{dis}}(\vec{K})$ calculated for Al and that calculated for the noble metals. Reasons for this difference were presented.

(iii) The analysis was generalized to real samples by including the effect of electron-impurity scattering on the relaxation time. The important parameter characterizing a sample was found to be the relative strengths of electron-dislocation scattering and electron-impurity scattering.

(iv) The results of the explicit calculation of $\tau_{\text{dis}}(\vec{K})$ were compared with previous empirical determinations. Excellent agreement was found between the theory and the empirical determinations of $\tau_{\text{dis}}(\vec{K})$ for measured samples of Al and Ag.

(v) The present results are shown to provide support for the recent theories of the effect of electron-dislocation scattering on the low-temperature electron-phonon and the electron-electron scattering contributions to the electrical resistivity.

ACKNOWLEDGMENT

We gratefully acknowledge the financial support provided by the Israel–United States Binational Science Foundation (BSF), Jerusalem, Israel.

APPENDIX

We want to justify Eq. (2.6) by showing that

$$[\vec{v}(\vec{K}_2) - \vec{v}(\vec{K}_1)]^2 \simeq (\hbar/m)^2 [\hbar^2 G^2 / 4m |w(G)|]^2 q^2, \quad (\text{A1})$$

for the case for which \vec{K}_1 and \vec{K}_2 lie very close to each other and also very close to the Brillouin-zone boundary of a polyvalent or noble metal. Thus, $\vec{q} = \vec{K}_2 - \vec{K}_1$ is a small quantity. The relevant geometry for a noble metal is given in Fig. 6. The geometry for a polyvalent metal is quite similar. The solid curve in the figure is the Fermi surface and the two dashed lines are the Brillouin-zone boundaries. The reciprocal-lattice vector \vec{G} connects the two plane waves needed to represent the pseudo-wave-function of both electron states \vec{K}_1 and \vec{K}_2 , and $w(G)$ is the corresponding screened, electron-ion pseudopotential matrix element. It is convenient to choose axes in \vec{K} space such that \vec{G} points in the z direction.

Since the velocity $\vec{v}(\vec{K})$ of the electron is given by the derivative of the energy $E(\vec{K})$, we begin by writing down the standard two-plane-wave expression¹⁷ for the energy of an electron in state \vec{K} ,

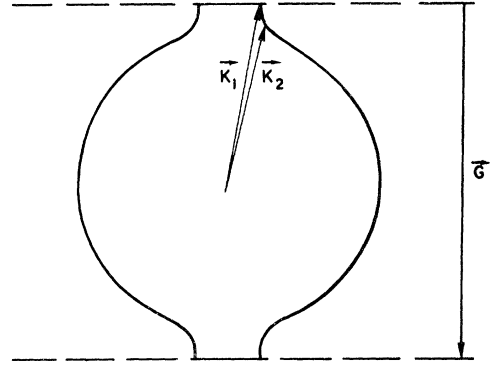


FIG. 6. Schematic plot of the cross section of the Fermi surface of a noble metal, showing the intersections of the Fermi surface (solid curve) with the Brillouin-zone boundaries (dashed lines) which are separated by the reciprocal-lattice vector \vec{G} . The initial and final electron states \vec{K}_1 and \vec{K}_2 lie in the nonspherical portion of the Fermi surface ("neck") near the Brillouin-zone boundary.

$$E(\vec{K}) = \frac{1}{2} \left[\frac{1}{2} (\vec{K} - \vec{G})^2 + \frac{1}{2} K^2 \right] - \frac{1}{2} \left\{ \left[\frac{1}{2} (\vec{K} - \vec{G})^2 - \frac{1}{2} K^2 \right]^2 + 4w^2 \right\}^{1/2}, \quad (\text{A2})$$

where the minus sign before the square root shows that we are dealing with the lower band. We have used atomic units ($\hbar = m = 1$) and introduced the abbreviated notation $w \equiv |w(G)|$. Since \vec{G} is in the z direction, the components of $\vec{v}(\vec{K})$ in the x and y directions are unaffected by the nonsphericity of the Fermi surface. Differentiation yields

$$v_x(\vec{K}) = \frac{\partial E(\vec{K})}{\partial K_x} = K_x, \quad (\text{A3})$$

$$v_y(\vec{K}) = \frac{\partial E(\vec{K})}{\partial K_y} = K_y.$$

However, in the z direction, the effect of the nonsphericity of the Fermi surface is crucial. Differentiation yields

$$v_z(\vec{K}) = \frac{\partial E(\vec{K})}{\partial K_z} = K_z - \frac{1}{2} G + \frac{1}{2} G \Delta_{\vec{K}} (\Delta_{\vec{K}}^2 + 16w^2)^{-1/2}, \quad (\text{A4})$$

where

$$\Delta_{\vec{K}} \equiv (\vec{K} - \vec{G})^2 - K^2. \quad (\text{A5})$$

We need $\vec{v}(\vec{K}_2) - \vec{v}(\vec{K}_1)$. The x and y com-

ponents are trivial:

$$\begin{aligned} v_x(\vec{K}_2) - v_x(\vec{K}_1) &= K_{2x} - K_{1x} = q_x, \\ v_y(\vec{K}_2) - v_y(\vec{K}_1) &= K_{2y} - K_{1y} = q_y. \end{aligned} \quad (\text{A6})$$

For the z component, we exploit the fact that q_z is a small quantity and make a Taylor expansion around K_{1z} to obtain

$$\begin{aligned} v_z(\vec{K}_2) - v_z(\vec{K}_1) &\simeq q_z [\partial v_z(\vec{K}_1) / \partial K_{1z}] \\ &= q_z [1 - 16G^2 w^2 (\Delta_{\vec{K}}^2 + 16w^2)^{-3/2}]. \end{aligned} \quad (\text{A7})$$

Thus far, the results apply to any initial electron state \vec{K}_1 . We now specialize the results to the case at hand for which \vec{K}_1 lies near the Brillouin-zone boundary. Thus, $K_{1z} \simeq \frac{1}{2}G$, implying that $\Delta_{\vec{K}} \simeq 0$.

This reduces (A7) to

$$v_z(\vec{K}_2) - v_z(\vec{K}_1) \simeq q_z (1 - G^2/4w). \quad (\text{A8})$$

Combining (A6) and (A8) yields the final result

$$\begin{aligned} &[\vec{v}(\vec{K}_2) - \vec{v}(\vec{K}_1)]^2 \\ &\simeq (\hbar/m)^2 q^2 \\ &\quad + (\hbar/m)^2 [\hbar^2 G^2 / 4m |w(G)|]^2 q_z^2, \end{aligned} \quad (\text{A9})$$

where we have ignored a small term and restored \hbar and m . Since the factor in brackets appearing in the q_z^2 term is of the order 10^2 , one may ignore the q^2 term unless \vec{q} happens to lie entirely in the x - y plane. Similarly, for a general direction of \vec{q} , the magnitudes of q_z^2 and q^2 are comparable. Ignoring the first term in (A9) and replacing q_z^2 by q^2 in the second term leads directly to Eq. (A1).

*On sabbatical leave at Cavendish Laboratory, University of Cambridge, England.

¹J. Bass, *Adv. Phys.* **21**, 431 (1972).

²M. R. Cimberle, G. Bobel, and C. Rizzuto, *Adv. Phys.* **23**, 699 (1974).

³J. A. Rowlands and S. B. Woods, *J. Phys. F* **5**, L100 (1975).

⁴H. van Kempen, J. S. Lass, J. H. J. M. Ribot, and P. Wyder, *Phys. Rev. Lett.* **37**, 1574 (1976).

⁵Y. Fujita and T. Ohtsura, *J. Low Temp. Phys.* **29**, 333 (1977).

⁶B. R. Barnard and A. D. Caplin, *Commun. Phys.* **2**, 223 (1977).

⁷J. A. Rowlands and S. B. Woods, *J. Phys. F* **8**, 1929 (1978).

⁸J. A. Rowlands, C. Duvvury, and S. B. Woods, *Phys. Rev. Lett.* **40**, 1201 (1978).

⁹B. R. Barnard and A. D. Caplin, *J. Phys. (Paris), Colloq.* **39**, C6-1050 (1978).

¹⁰B. Levy, M. Sinvani, and A. J. Greenfield, *Phys. Rev. Lett.* **43**, 1822 (1979).

¹¹T. Endo and T. Kino, *Jpn. J. Phys. Soc.* **46**, 1515 (1979).

¹²M. Sinvani, A. J. Greenfield, A. Bergmann, M. Kaveh, and N. Wiser, *J. Phys. F* **11**, 149 (1981).

¹³J. S. Dugdale and Z. S. Basinski, *Phys. Rev.* **157**, 552 (1967).

¹⁴A. Bergmann, M. Kaveh, and N. Wiser, *J. Phys. F* **10**, L71 (1980).

¹⁵A. Bergmann, M. Kaveh, and N. Wiser, *Solid State Commun.* **34**, 369 (1980).

¹⁶M. Kaveh and N. Wiser, *J. Phys. F* **10**, L37 (1980).

¹⁷J. M. Ziman, *Electrons and Phonons* (Clarendon, Oxford, 1960).

ford, 1960).

¹⁸Y. K. Chang and R. J. Higgins, *Phys. Rev. B* **12**, 4261 (1975).

¹⁹B. R. Watts, *J. Phys. F* **7**, 939 (1977); R. A. Brown, *ibid.* **8**, 1159 (1978); E. Mann, *ibid.* **9**, L135 (1979).

²⁰Y. Bergman, M. Kaveh, and N. Wiser, *Phys. Rev. Lett.* **32**, 606 (1974).

²¹M. Kaveh and N. Wiser, *Phys. Rev. B* **21**, 2278 (1980); **21**, 2291 (1980).

²²R. S. Sorbello, *J. Phys. F* **4**, 503 (1974).

²³A. Bergmann, M. Kaveh, and N. Wiser, *J. Phys. F* (in press).

²⁴N. W. Ashcroft, *Philos. Mag.* **8**, 2055 (1963).

²⁵J. M. Ziman, *Adv. Phys.* **10**, 1 (1961).

²⁶R. S. Sorbello, *Solid State Commun.* **12**, 287 (1973).

²⁷The curve that appears in that figure is simply a free-hand curve drawn through the points to guide the eye.

²⁸W. E. Lawrence and J. W. Wilkins, *Phys. Rev. B* **7**, 2317 (1973).

²⁹W. E. Lawrence, *Phys. Rev. B* **13**, 5316 (1976).

³⁰J. E. Black, *Can. J. Phys.* **56**, 708 (1978).

³¹J. H. J. M. Ribot, J. Bass, H. van Kempen, and P. Wyder, *J. Phys. F* **9**, L117 (1979).

³²M. Khoshnevisan, W. P. Pratt, P. A. Schroeder, S. Steenwyk, and C. Uher, *J. Phys. F* **9**, L1 (1979).

³³M. Danino, M. Kaveh, and N. Wiser, *J. Phys. F* **11**, L107 (1981).

³⁴M. Sinvani, A. J. Greenfield, M. Danino, M. Kaveh, and N. Wiser, *J. Phys. F* **11**, L73 (1981).

³⁵M. Danino, M. Kaveh, and N. Wiser, *J. Phys. F* (in press).

³⁶M. Brody, M. Kaveh, and N. Wiser, *Physica B* **108**, 1165 (1981).